Nitrate, nitrite, and nitrous oxide transformations in sediments along a salinity gradient in the Weser Estuary

Michael Nielsen[1,3,*], Armin Gieseke[2], Dirk de Beer[2], Niels Peter Revsbech[1]

[1]Department of Biological Sciences, Microbiology, University of Aarhus, 8000 Aarhus C, Denmark
[2]Max Planck Institute for Marine Microbiology, 28359 Bremen, Germany

[3]*Present address:* Department of Civil Engineering, National University of Ireland, Galway, Ireland

ABSTRACT: The dynamics of the nitrogen intermediates N_2O and NO_2^- in estuarine sediments were studied along a salinity gradient in the eutrophied Weser Estuary (Germany) using microsensors for N_2O, NO_2^-, NO_x^-, and O_2. During dark incubations in the laboratory of sediment samples from a freshwater site, a brackish water site with fluctuating salinity, and a marine site, the effects of environmental changes in nitrogen availability and salinity on microscale sediment dynamics were examined. Generally, sediment levels of intermediates were low: 1 to 25 µM NO_2^- and 0 to 8 µM N_2O. However, significant variation was found in accumulation patterns and in the potential of the residing microbial community to control sediment releases of the intermediates. At fresh- and brackish water sites, NO_2^- production was found in the anoxic denitrification zone, and release from the sediments was effectively prevented by activity of nitrite oxidisers in oxic surface layers. In contrast, high rates of NO_2^- release occurred in marine sediment, where NO_2^- production was predominantly associated with incomplete nitrification in oxic layers. Similarly, stimulated partial nitrification due to NH_4^+ addition led to NO_2^- liberation from brackish water sediment. Production of N_2O was never observed in sediment from the brackish water site, which is naturally exposed to a daily regime of water column variations, but transient N_2O accumulation was observed in the other sediments. The production of N_2O could be induced by an abrupt change in either NO_3^- or salinity, and was found in anoxic or micro-oxic sediment layers. Because oxic sediment layers showed little or no potential for N_2O consumption (in contrast to NO_2^-) the accumulation of N_2O always resulted in release from the sediment surface. Results demonstrate that changes in environmental parameters such as salinity and NO_3^- can trigger sediment production and release of NO_2^- and N_2O, but further suggest that microbial sediment communities are highly adaptive and can become resistant towards intermediate release when regularly exposed to fluctuating conditions.

KEY WORDS: Nitrite · Nitrous oxide · Sediment · Denitrification · Nitrification · Emission

INTRODUCTION

Estuaries are active sites for reduction of the inorganic nitrogen pool in river waters and play an important role in limiting the nitrogen input to marine environments (Ogilvie et al. 1997). However, associated with high nitrogen turnover rates is the increased risk of production of the nitrogen intermediates nitrite (NO_2^-) and nitrous oxide (N_2O), which is a concern due to their potentially harmful effects on the environment.

NO_2^- is toxic and adversely affects aquatic organisms at relatively low concentrations. For example, certain groups of sediment-dwelling invertebrates are harmed by NO_2^- concentrations between 10 and 20 µM (Neumann et al. 2001, Kelso et al. 1999b), and European Union guidelines recommend NO_2^- concentrations below 0.25 µM in waters that support salmonid fishes (European Economic Community 1978). N_2O oxide, on the other hand, is an aggressive greenhouse gas with a warming potential 200 to 300 times greater than CO_2

(Kramlich & Linak 1994) and, furthermore, is the dominant source for stratospheric NO radicals that are causing ozone layer destruction (Conrad 1996). Estuarine environments have been estimated to contribute about 60% of global marine N_2O production (Bange et al. 1996), and for NO_2^-, water-phase concentrations up to 140 µM have been reported (Dong et al. 2002).

The dynamics of NO_2^- and N_2O in sediments are complex, and the set of factors that control their accumulation and subsequent release to the water phase or to the atmosphere (N_2O) are not fully resolved. There are several aerobic and anaerobic microbial processes that produce nitrogen intermediates, and a range of environmental parameters affect their accumulation, while microbial interactions may further regulate their release. NO_2^- is an intermediate of nitrification, denitrification, and dissimilatory nitrate reduction to ammonium (DNRA), while N_2O is an intermediate of denitrification and nitrifier-denitrification, and is formed as a by-product during nitrification and DNRA (Wrage et al. 2001, de Bie et al. 2002, Philips et al. 2002). Despite several potential sources, NO_2^- and N_2O are usually found in low concentrations, illustrating that microbial sediment communities are usually finely tuned to prevent significant accumulation and release. Nitrification and denitrification are recognized as the primary processes responsible for the generation of intermediates in sediments, although reports also exist on the contribution from DNRA (Kelso et al. 1997). In the case of nitrification, NO_2^- will accumulate if NO_2^- oxidation is slower than ammonia oxidation, which can be related to existing population numbers, availability of ammonium (NH_4^+) and NO_2^- as electron-donors, oxygen status, and inhibitory compounds (Venterea & Rolston 2000). Both NO_2^- and N_2O can accumulate by incomplete denitrification because of kinetic limitations on a community (Holtan-Hartwig et al. 2000) or enzyme level (Betlach & Tiedje 1981).

Elevated production of NO_2^- and N_2O appear strongly linked to nitrogen availability, which may reflect why build-ups are usually observed in eutrophic environments. Oxygen is equally considered to have a strong regulating effect (i.e. de Bie et al. 2002). Low oxygen levels may trigger production of N_2O and NO_2^- from nitrification as well as N_2O from denitrification, and can stimulate sediment release of NO_2^- produced in anoxic layers (Stief et al. 2002). Other known regulatory abiotic factors include temperature, pH, organics, NH_4^+ (for NO_2^-), and NO_2^- (for N_2O). Further, it has been proposed that temporal variation in environmental parameters (i.e. oxygen and nitrogen) can markedly enhance the production of intermediates (Robinson et al. 1998, Naqvi et al. 2000, Laursen & Seitzinger 2004). Therefore, tidally induced fluctuations in physicochemical parameters in estuar-

ine sediments may result in temporally increased NO_2^- and N_2O concentrations and subsequent release to the water column or atmosphere. In a recent microsensor study of nitrogen dynamics in subtropical estuarine sediment, occurrence of enhanced production and release of NO_2^- and N_2O was thus demonstrated in response to excessive loading with either NO_3^- or NH_4^+ (Meyer et al. 2008).

We hypothesize that change in environmental parameters such as increased availability of NO_3^- and NH_4^+ or rapid changes in salinity may cause imbalances in the sequential nitrogen conversions leading to enhanced production of NO_2^- and N_2O in estuarine sediment. The Weser estuary was chosen to study the effect of such environmental disturbances, as tidal cycles in this system expose the sediments to highly variable salinity and nutrient regimes. We further expect that a site regularly exposed to tidally induced salinity variations will be the most resistant to release of nitrogen intermediates due to the adaptive capacity of present microbial populations. Our work was facilitated by the use of microsensors that allow O_2, N_2O, NO_2^-, and NO_x^- concentrations to be measured at high spatial resolution within the sediment. The use of microscale biosensors for NO_2^-, and NO_x^- made it possible to analyse these ions in a saline environment. It was not our intention to replicate in detail the *in situ* conditions but to illustrate aspects of nitrogen intermediate dynamics at a microscale when estuarine sediments are exposed to a change in salinity or nitrogen loading.

MATERIALS AND METHODS

Study area. The Weser estuary (Germany) stretches more than 80 km from the city of Bremen to beyond Bremerhaven where it merges into the German Bight (see Fig. 1). The estuary receives water from the river Weser and its tributaries and has a mean water discharge of 317 $m^3 s^{-1}$. The Weser system is nutrient-rich with high water concentrations of inorganic nitrogen, primarily found as NO_3^-. A surveillance program for the Weser river and estuary dates back to 1979 (data available at http://fgg-weser.de/download_nue.html). At Brake, about 40 km downstream of Bremen, the water NO_3^- concentration ranged between 115 and 460 µM in 2004 to 2006, with minimum levels in late summer and maximum levels during winter. During the same period, water concentrations of NO_2^- and NH_4^+ were always below 3 and 10 µM, respectively. The estuary has a mean tidal range of about 3.5 m with the intrusion of high salinity, lower nutrient water from the German Bight (Beddig et al. 1997). Areas that stretch about 50 to 70 km downstream of Bremen are

exposed to strong diurnal variation in salinity of about 2 to 15‰ (Grabemann et al. 1997).

Sampling and experimental setup. Sediment samples were collected during early fall (September) from 3 locations along the Weser Estuary: a freshwater site, a brackish water site with diurnal fluctuations in salinity, and a marine site (Fig. 1). Prior to sampling, the salinity regime was surveyed at the brackish water location during a full tidal cycle, and observed to vary between 2 and 12‰. On the day of sediment collection, water samples were taken to determine *in situ* NO_3^- concentrations. Sediment sampling was performed at low tide on exposed tidal flats with fine particulate sediment material, and the ~10 cm deep samples were collected with a rectangular Plexiglas sampler that fit the flow cells (12×8 cm) used for sediment incubations in the laboratory. At the sampling locations, the sediment samples were carefully transferred to flow cells without destroying the layered architecture. They were then brought back to the laboratory, where they were connected to 60 l water reservoirs. Recirculating water (flow rate ~20 l h^{-1}) was prepared from artificial sea salt (Preis-Meersalz, Preis Aquaristik) and deionized water, and adjusted to salinity levels of 0.5, 6.5, and 25 g l^{-1}. $NaNO_3$ and NH_4Cl were supplemented from stock solutions to obtain various NO_3^- and NH_4^+ concentrations in the water phase. During the 10 d experimental period, the flow systems

Fig. 1. Weser estuary sampling locations. Freshwater (1•), brackish water (2•), and marine (3•) sites

were kept in the dark to prevent photosynthetic activity. Temperature was kept at 22.5 ± 1°C, corresponding to mid-summer *in situ* temperature. The salinity was measured routinely and adjusted through additions of deionized water to compensate for evaporative losses. Every day, 10 ml filtered water samples were taken from each system to determine water phase concentrations of NO_3^- and NH_4^+. Concentrations of NO_3^- (+NO_2^-) were measured with a macroscale version of a NO_x^- biosensor (Unisense A/S) whereas NH_4^+ concentrations were determined using a conventional spectrophotometric method (Keeney & Nelson 1982).

Microprofiles of each parameter were measured separately with microsensors mounted on a computer-controlled micro-manipulator for automatic profiling. Through a computer interface (ADC-216USB and Profix software, Unisense A/S) it was possible to program important profiling settings including step size, sensor resting time at each profile depth, and maximum profile depth. A step size of 200 µm was used for O_2 profiles, whereas 400 or 800 µm was used for NO_2^-, NO_x^-, and N_2O profiles. Larger steps for the latter profiles were chosen because of the relatively long sensor response times that necessitated similar long resting times (45 to 75 s) at each depth. A dissection microscope was used to determine the position of the sediment–water interface before each profile measurement.

Microsensors. Microsensors for NO_2^-, NO_x^-, N_2O, and O_2 were prepared and calibrated as described previously (Revsbech 1989, Larsen et al. 1997, Andersen et al. 2001, Nielsen et al. 2004). The NO_2^- and NO_x^- micro-biosensors had tip diameters of about 50 to 80 µm and had 90% response times of between 45 and 75 s. Electrophoretic sensitivity control (ESC) was used to control sensitivity of the biosensors (Kjær et al. 1999), which made it possible to measure NO_2^- and NO_x^- concentrations down to about 0.2 µM. As the NO_x^- and NO_2^- biosensors are also sensitive to N_2O, the response to N_2O was quantified so that it was possible to correct for N_2O interference on the signal. The N_2O microsensors had detection limits of about 0.3 µM N_2O. The 90% response time of 40 to 50 µm thick sensors was about 30 s.

A modified version of the diffusivity sensor described by Revsbech et al. (1998), based on outflux of N_2O instead of H_2, was used to determine the effective diffusion coefficient (ϕD_s). The sediment samples for diffusivity determinations were incubated overnight with 20% acetylene in the NO_x^--free water phase to inhibit N_2O transformations during the measurements. To integrate over a representative volume, diffusivity sensors should have diameters of at least 3 times the average sediment grain size. The diffusivity sensor was therefore manufactured with a tip diameter of 0.8 mm,
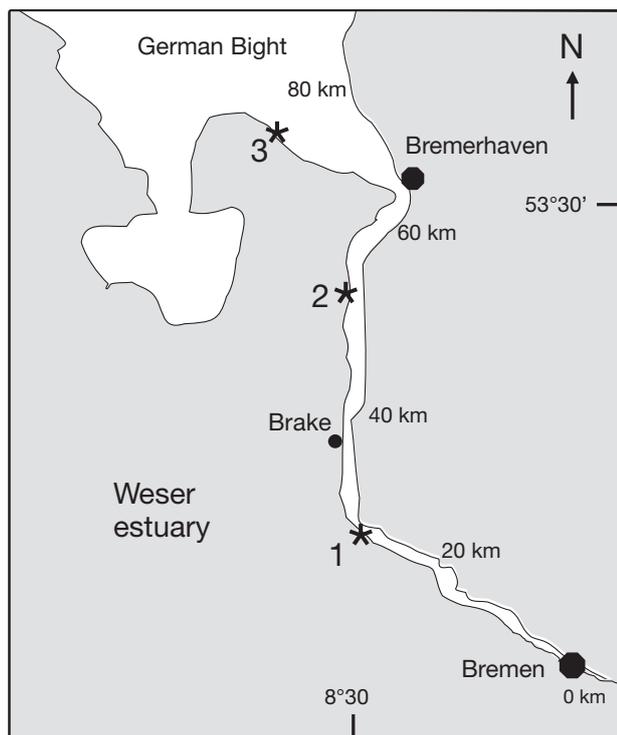
but the inferior spatial resolution given by the large size did not allow for recording of detailed diffusivity microprofiles. Instead, triplicate determinations at a depth of about 3 mm were performed. Calibration was performed in 40 to 60 μm glass bead sediment and 1% agar (Revsbech et al. 1998).

Profile interpretation. NO_3^- concentration profiles were calculated by subtracting the mean local NO_2^- concentrations from local NO_x^- concentrations. At conditions where N_2O was detected in the sediment, NO_3^- and NO_2^- profiles were further corrected. The part of NO_2^- and NO_x^- biosensor signals that was related to N_2O was calculated using measured mean local N_2O concentrations and biosensor N_2O calibration values.

Flux rates across the sediment–water interface were calculated from concentration gradients in the uppermost sediment layer using Fick's first law of diffusion, $J = -\phi D_s \, dC/dx$, where J is the flux, ϕ the porosity, D_s the diffusion coefficient, and dC/dx the concentration gradient. Directly measured values for ϕD_s were used for the flux calculations, where diffusion coefficients for ions in the sediments relative to the values in water were assumed to be reduced with the same percentage as determined for gas (N_2O). The diffusivities for NO_2^- and NO_3^- were set to 79% of the value for O_2 (Li & Gregory 1974), and the diffusivity for N_2O was identical (within 0.5%) to that of O_2 (Broecker & Peng 1974). Activity profiles in the sediment were calculated from the profile simulation program 'Profile' (Berg et al. 1998). Mean concentration values of 3 different profiles were used for activity calculations. By modeling NO_x^- (i.e. $NO_2^- + NO_3^-$) profiles it is possible to estimate depth profiles of production (i.e. oxidation of NH_4^+) and consumption of NO_x^-.

Experiments. In steady-state experiments, the sediment distributions of NO_2^-, NO_x^-, N_2O, and O_2 were examined for all samples with approximately 10 or 200 μM NO_3^- in the water phase (Table 1). The low concentration of 10 μM allowed precise modelling of nitrification activities where modelling at high NO_3^-

may be less accurate. In sediment from the brackish water site, concentration profiles were also measured in the presence of 50 μM NH_4^+ plus 200 μM NO_3^-. For each experimental condition, a minimum incubation time of 16 h was used following a change in water phase concentration to ensure that gradients in the sediment had approached equilibrium when the measurements were performed. For all analysed conditions, 3 replicate profiles of each parameter were recorded. Additionally, during the transition in water phase concentration from 10 to 200 μM NO_3^- in sediment from the brackish water site, single profiles of NO_2^- and N_2O were measured at 0, 1, 3, 5, and 17 h.

In perturbation experiments, the different samples were exposed to abrupt changes in salinity and NO_3^- concentration in the overlying water phase (Table 1), corresponding to changes that might happen between low and high tide. In 2 independent perturbation events, sediment from the brackish water site, incubated with 200 μM NO_3^-, was exposed to 0.5‰ water with 200 μM NO_3^- and to 25‰ water with 10 μM NO_3^-. Similarly, sediment incubated with 200 μM NO_3^- and marine sediment incubated with 10 μM NO_3^- were exposed to 6.5‰ water with 200 μM NO_3^-. During each perturbation event, single profiles of N_2O and O_2 were measured at 0, 1, 2, 4, 6, and 9 h. In freshwater sediment in which N_2O was found beyond 9 h, the duration of the perturbation experiment was extended to 31 h. NO_2^- and NO_x^- profiles were only measured at 0 and 9 h during salinity perturbations (data not shown) as the biosensor signals are salinity-dependent (Nielsen et al. 2004) and thus do not allow accurate analysis in the presence of a steep salinity gradient.

Sediment core samples were taken from the flow cells for characterisation of porosities, organic C content, and C:N ratios in the upper 5 mm. Porosities were determined by drying 5 mm thick sediment slices at 105°C for 24 h with subsequent determination of water loss. Organic C contents and C:N ratios were determined with a Carlo-Erba CN analyser.

Table 1. Nitrogen intermediate concentrations and salinities used in steady-state and perturbation experiments conducted with sediment samples from the 3 sites along the salinity gradient. (→): Change in salinity and NO_3^- concentration. nd: not determined

	Freshwater	Brackish water	Marine
Steady-state			
NO_3^- (μM)	10	10	10
NO_3^- (μM)	200	200	200
NO_3^- (μM) + NH_4^+ (μM)	nd	200 + 50	nd
Perturbation			
Salinity (ppt)/NO_3^- (μM)		6.5/10 → 6.5/200	
	0.5/200 → 6.5/200	6.5/200 → 0.5/200	25/10 → 6.5/200
		6.5/200 → 25/10	

RESULTS

Sediment characteristics

At all sampling locations, the sediments were silty with porosities in the upper 5 mm of 0.60, 0.73, and 0.72 for freshwater, brackish water and marine sediments, respectively. The organic C contents were determined to be 11, 21 and 23 mg g^{-1} dry weight, respectively, and the organic C:N ratios were about 25 (21, 24 and 27, respectively). The ϕD_s values (for O_2 or N_2O diffusion in the matrix) at 22.5°C were 1.01, 1.15, and 0.95×10^{-5} cm^2 s^{-1}, respectively. Using the conversion factor of 0.79 between gas and the ions in question, this corresponds to ϕD_s values for NO_2^- or NO_3^- in the samples of 0.80, 0.91, and 0.75×10^{-5} cm^2 s^{-1}, respectively.

Water phase NO_3^- and NH_4^+ concentrations

Analyses of water samples taken at the day of sediment collection showed *in situ* NO_3^- concentrations for freshwater, brackish water and marine sediments of about 160, 150, and 50 μM, respectively. Sampling at low tide explained the similar *in situ* water NO_3^- concentrations at the first 2 sampling locations and the relatively high concentration at the marine site. Water phase NO_3^- concentrations in the incubation systems during steady-state experiments varied between 9 and 14 μM for low NO_3^- incubations and between 170 and 190 μM for high NO_3^- incubations. The NH_4^+ concentration in the water phase remained low (<4 μM) in sediment samples from fresh- and brackish water sites during the experimental period, except when the water above the sediment from the brackish water site was supplemented with NH_4^+ (47 μM). In the water column above the marine sediment, there was a continuous increase in NH_4^+ concentrations, reaching a maximum level of 28 μM corresponding to an average sediment NH_4^+ efflux of about 24 pmol cm^{-2} s^{-1}.

NO_2^- and NO_3^- at steady state conditions

Concentration profiles of NO_2^-, NO_3^-, N_2O, and O_2 at conditions with either 10 μM NO_3^-, 200 μM NO_3^-, or 200 μM NO_3^- plus 50 μM NH_4^+ (brackish water sediment) in the water phase are presented as means of 3 replicates (see Figs. 2 to 5). As the error bars indicate, distributions of the different nitrogen forms were characterized by some degree of heterogeneity between replicate measurements.

At low NO_3^- concentrations (~10 μM) in the overlying water phase, distributions of NO_2^-, NO_3^-, and O_2 were similar in fresh- and brackish water sediments (Figs. 2a,b & 3a,b). In both sediment types, O_2 penetrated to depths of about 3 mm. Distinct NO_3^- production zones were found in oxic layers, with concentration peaks of 21 μM in the freshwater sediment and 19 μM in sediment from the brackish water site. The highest NO_3^- production rates were observed just above the oxic–anoxic interface, whereas NO_3^- reduction occurred in deeper anoxic layers. In both sediment types, there was an efflux of NO_3^- to the water phase. Sediment NO_2^- concentrations were low, with maximum peaks of about 1 μM (freshwater) and 2.5 μM brackish water found within anoxic NO_3^- reduction zones. Anaerobically produced NO_2^- was consumed in deeper anoxic layers and in oxic surface layers just above the oxic–anoxic interface. In marine sediment, the O_2 penetration depth was less than 2 mm (Fig. 4a,b). Aerobic NO_3^- production resulted in a concentration peak of about 20 μM within the oxic layer. In contrast to the other samples, the NO_2^- distribution profile in marine sediment was characterized by a distinct aerobic production zone that resulted in NO_2^- accumulation to about 10 μM. Aerobically produced NO_2^- (and NO_3^-) was partly consumed within the marine sediment, and there was a NO_2^- efflux of about 0.71 pmol cm^{-2} s^{-1} (Table 2).

Increasing the NO_3^- concentration in the water from 10 to 200 μM did not affect the O_2 penetration depth in any of the samples, but resulted in significant changes in sediment distributions of NO_2^- and NO_3^-. The flux of NO_3^- from the water to the sediment was stimulated by the elevated NO_3^- concentration, and the increased supply to anoxic layers resulted in higher rates of anaerobic NO_3^- reduction (Table 3). However, the effect on NO_3^- penetration depth was highly variable. In freshwater sediment (Fig. 2c,d), NO_3^- penetration was largely unaltered (~4 mm), whereas the penetration depth in brackish water (Fig. 3c,d) and marine (Fig. 4c,d) sediments increased from 5 to 11.5 mm and from 2.6 to 4 mm, respectively. From the microprofiles, we calculated for all samples a pronounced stimulation of nitrification with increased rates of aerobic NH_4^+ oxidation and NO_3^- production when comparing activities during incubations with 10 and 200 μM (Table 3, Figs. 2 to 4). Increased NO_3^- supply to the sediment also stimulated net anaerobic NO_2^- formation. In freshwater sediment, the anoxic NO_2^- peak increased from 1 to 3 μM, whereas the deep NO_3^- penetration in sediment from the brackish water site resulted in a 5 mm broad NO_2^- production zone and increased the anoxic NO_2^- peak from 2.5 to 15 μM. The increased rates of net anaerobic NO_2^- production in fresh- and brackish water sediments did not lead to an elevated NO_2^- efflux from the sediments, as the produced NO_2^- in both cases was
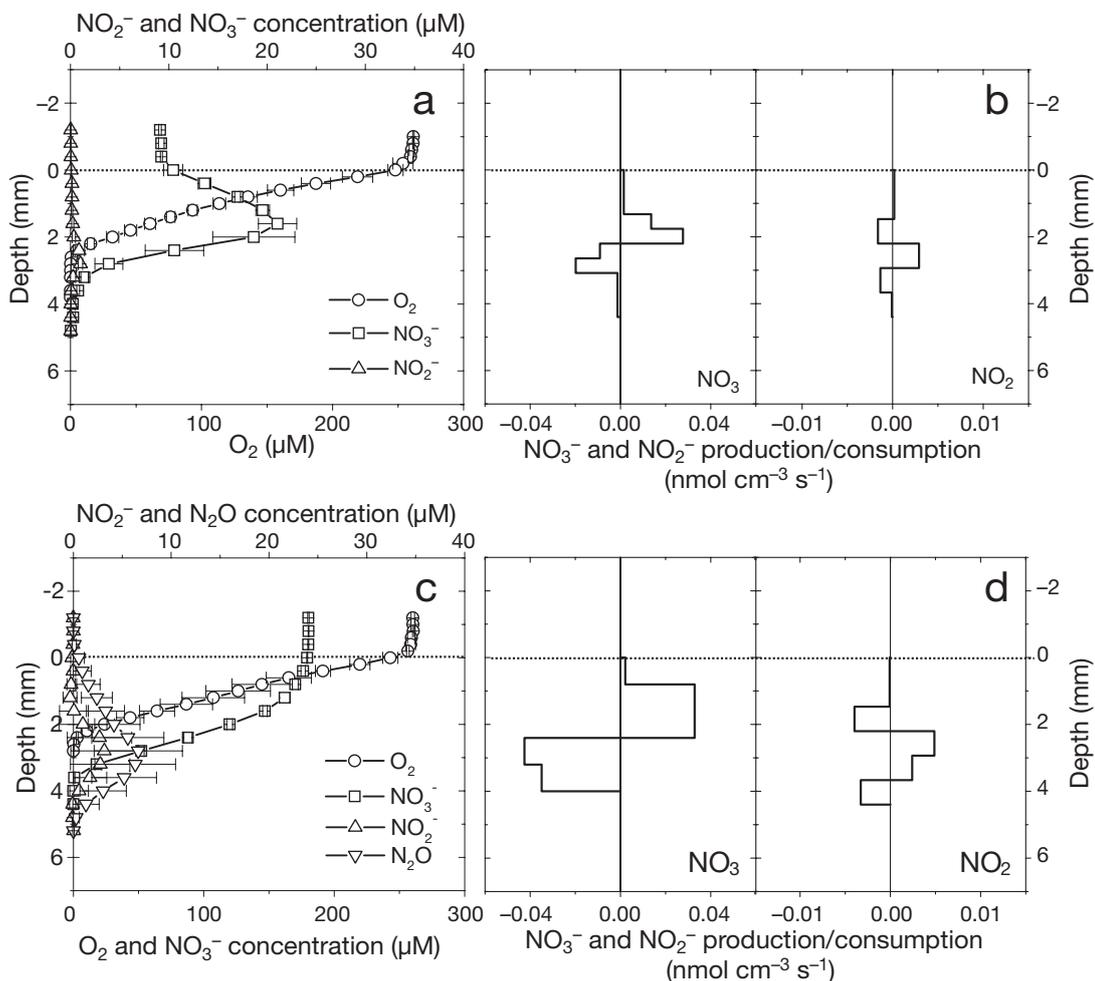
Fig. 2. Average concentration profiles of N_2O, NO_2^-, NO_3^-, and O_2, and reaction rates of NO_2^- and NO_3^- in freshwater sediment (means ± SD). Incubations of (a, b) 10 µM and (c, d) 200 µM NO_3^-. The dotted lines indicate the sediment surface

consumed in the oxic sediment layers before it could reach the water phase. In marine sediment, there was a large increase in aerobic NO_2^- production, although no apparent stimulation of anaerobic NO_2^- formation occurred; the NO_2^- peak in the sediment increased from 10 to 26 µM with a comcomitant increase in the efflux of NO_2^- from 0.71 to 2.26 pmol cm^{-2} s^{-1} (Table 2). The calculated net areal NO_2^- production rates in anoxic layers (at 200 µM NO_3^-) varied by a factor of 10 and were 0.00054, 0.0012, and 0.00012 nmol cm^{-2} s^{-1} for freshwater, brackish water, and marine sediments, respectively.

Supplementation with NH_4^+

Increasing the NH_4^+ concentration in the water phase overlying sediment from the brackish water site from 3 to 47 µM was followed by significant changes in NO_2^- and NO_3^- profiles due to marked stimulation of the nitrification process (Table 3, Fig. 5). The increased rates of NH_4^+ and NO_2^- oxidations resulted in a sub-surface NO_3^- peak and turned the sediment into a source of NO_2^- to the water phase, with an efflux rate of 0.49 pmol cm^{-2} s^{-1} (Table 2). Anaerobic NO_3^- reduction and NO_2^- production rates were similar with and without NH_4^+ addition (Table 3, Figs. 3 & 5), but the change in overall gradients led to increased concentrations of NO_2^- with a concentration peak of 20 µM.

N_2O formation at constant salinity

Sediment N_2O concentrations in the different samples during steady-state incubations were generally below the sensor detection limit of about 0.3 µM. N_2O could, however, be detected in freshwater sediment when incubated with 200 µM NO_3^- in the water phase (Fig. 2). Under this condition, net N_2O production was
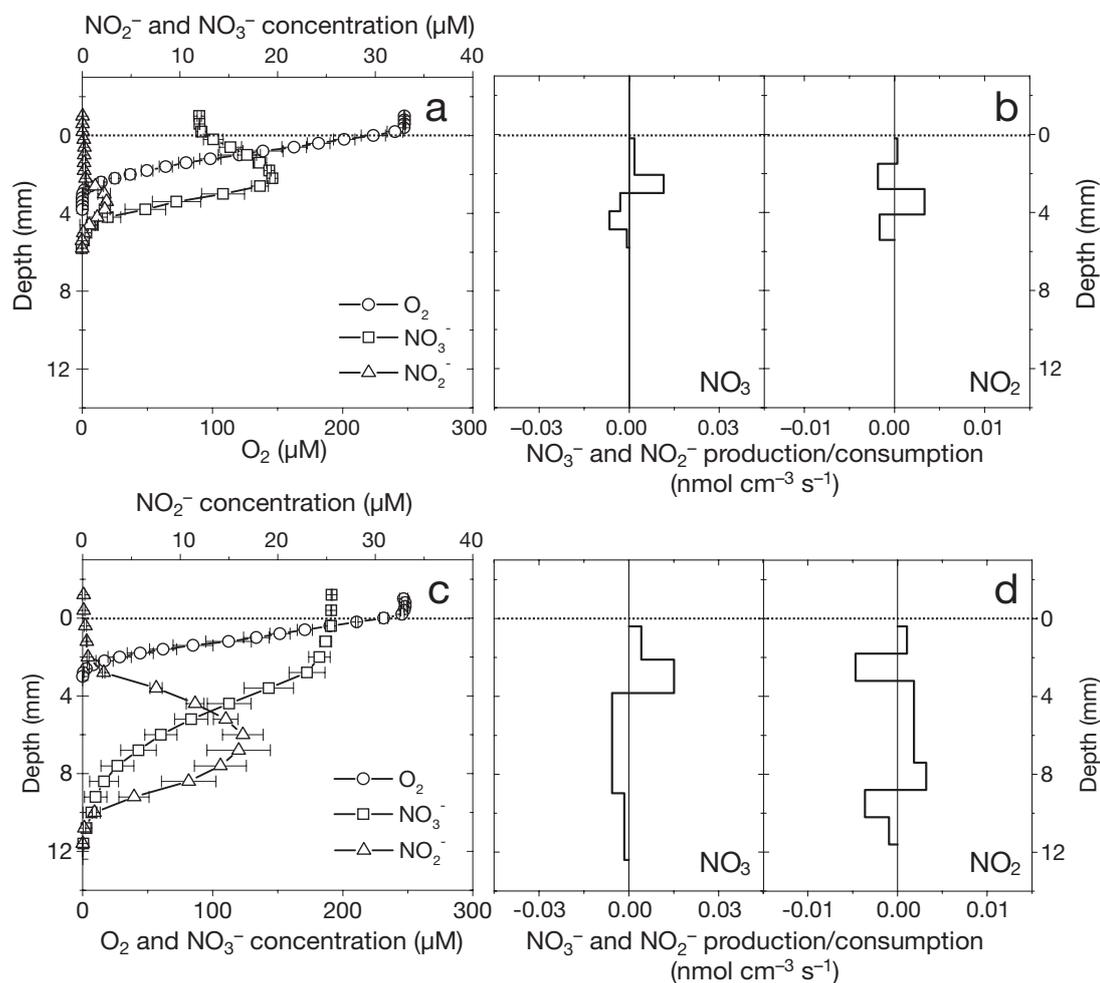
Fig. 3. Average concentration profiles of NO_2^-, NO_3^- and O_2, and reaction rates of NO_2^- and NO_3^- in sediment from the brackish water site (means ± SD). Incubations of (a, b) 10 µM and (c, d) 200 µM NO_3^-. The dotted lines indicate the sediment surface. N_2O concentrations were always below detection limit

observed in anoxic sediment layers just below the oxic–anoxic interface, but N_2O production was highly variable, with concentration peaks between 3 and 12 µM N_2O among the 3 replicates. Net N_2O production in the anoxic sediment layer was followed by

release of N_2O from the sediment to the overlying water with an average efflux of 0.16 pmol N_2O cm^{-2} s^{-1} (Table 2). The accumulation of N_2O was a transient phenomenon; N_2O was undetectable in the sediment 48 h after the profiles were measured.

Table 2. Efflux rates of NO_2^- and N_2O (pmol cm^{-2} s^{-1}) from the sediment surface under different experimental conditions, calculated from concentration gradients in the uppermost sediment layers. Unless indicated otherwise, values are mean ± SD of 3 replicates. nd: no data, no significant efflux rates were observed

Expt.	Freshwater	Intermediate	Marine
Steady-state			
10 µM NO_3^-	nd	nd	0.71 ± 0.04 (NO_2^-)
200 µM NO_3^-	0.16 ± 0.08 (N_2O)	nd	2.26 ± 0.20 (NO_2^-)
200 µM NO_3^-/ 50µM NH_4^+	nd	0.49 ± 0.05 (NO_2^-)	nd
Perturbation			
N_2O, max. rate	0.072	nd	0.075

Table 3. Calculated net NH_4^+ oxidation and NO_3^- reduction rates in sediment samples under different incubation conditions during steady-state experiments

Reduction rates (pmol cm^{-2} s^{-1})	Freshwater	Brackish water	Marine
NH_4^+-oxidation			
10 µM NO_3^-	1.9	1.2	4.2
200 µM NO_3^-	5.2	2.8	7.5
200 µM NO_3^-/50 µM NH_4^+		5.1	
NO_3^--reduction			
10 µM NO_3^-	1.5	1.0	1.4
200 µM NO_3^-	6.2	3.4	6.1
200 µM NO_3^-/50 µM NH_4^+		3.1	

NO_3^- perturbation at constant salinity

The sediment NO_2^- and N_2O dynamics from the brackish water site were also monitored during a transition phase, when the water NO_3^- concentration was elevated from 12 to 190 µM (Fig. 6). While N_2O remained undetectable throughout, there was a gradual build-up of NO_2^- in the anoxic sediment layer, with the peak concentration rising from 3 to 16 µM within the 17 h experimental period. At the same time, gradual changes in depth and width of the NO_2^- production zone took place, which resulted in a distinct displacement of the NO_2^- peak in the sediment from about 3.5 to 6 mm depth.
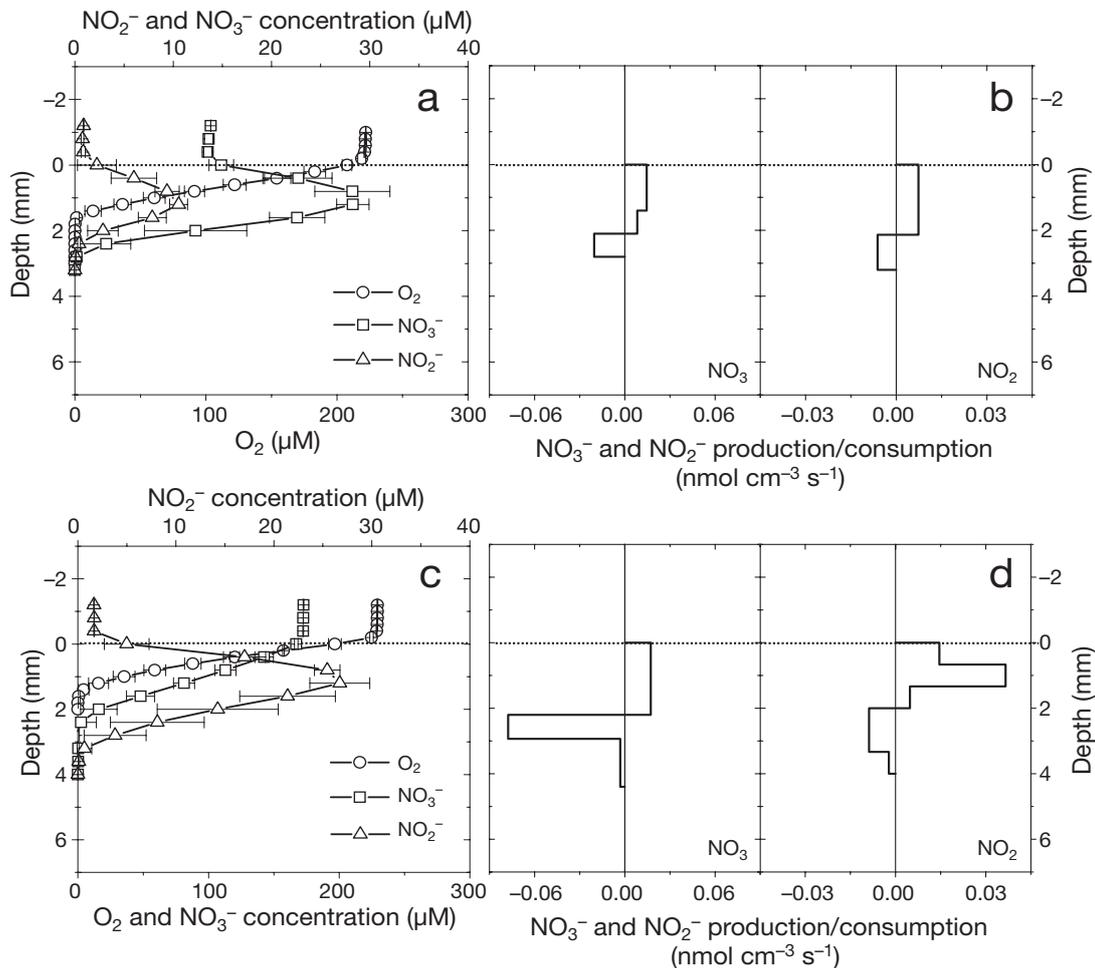

Fig. 4. Average concentration profiles of NO_2^-, NO_3^- and O_2, and reaction rates of NO_2^- and NO_3^- in marine sediment (mean ± SD). Incubations of (a, b) 10 µM and (c, d) 200 µM NO_3^-. The dotted lines indicate the sediment surface. N_2O concentrations were always below detection limit
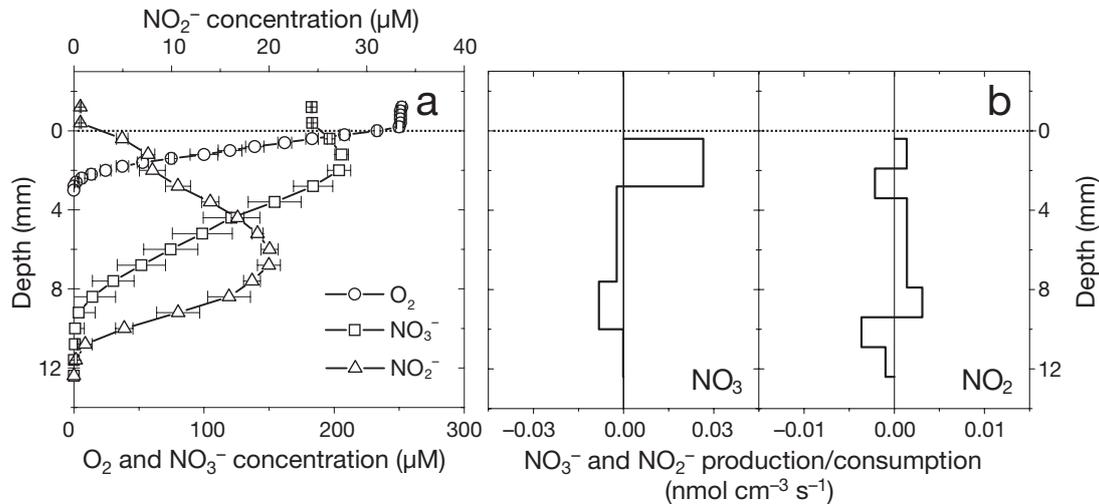
Fig. 5. (a) Average concentration profiles of NO_2^-, NO_3^- and O_2, and (b) reaction rates of NO_2^- and NO_3^- in sediment from the brackish water site at incubation conditions of 200 µM NO_3^- and 47 µM NH_4^+ in the water phase (means ± SD). The dotted lines indicate the sediment surface. N_2O concentrations were always below detection limit

Salinity perturbations

Perturbation experiments with an abrupt change in water phase salinity (Table 1) caused N_2O to accumulate in freshwater and marine sediments (Fig. 7a,c), but never in sediment from the brackish water site (data not shown). During salinity perturbations, no distinct change in O_2 penetration depths could be identified (Fig. 7b,d). The N_2O production zone in freshwater sediment was found below the oxic–anoxic interface, and the highest N_2O concentration (4 µM) was encountered 9 h after the onset of the salinity increase (Fig. 7a). N_2O was still detectable (2 µM) after 31 h. In

marine sediment, the N_2O production zone was located at or just below the oxic–anoxic interface (Fig. 7c). The N_2O dynamics in marine sediment were faster, and the maximum N_2O concentration encountered was about 2 µM. Build-up to the highest level took place within the first 2 h after the decrease in salinity, and after 9 h the N_2O peak had almost disappeared again. In both freshwater and marine samples, the transient build-up resulted in N_2O release from the sediment surface with almost identical maximum rates of 0.072 and 0.075 pmol N_2O cm^{-2} s^{-1}, respectively (Table 2).

DISCUSSION

Until recently, it was not possible to measure NO_2^- and N_2O at high spatial resolution in marine environments; consequently, very few studies have addressed factors that control the production and accumulation of N_2O and NO_2^- at a microscale in marine sediments (Meyer et al. 2005, 2008). Once acclimatized (for a few hours) to the salinity level of the sample, biosensors for NO_2^- and NO_x^- are not prone to interference from high concentrations of salts, in contrast to liquid ion exchange (LIX) microsensors for NH_4^+, NO_2^-, and NO_3^-, which cannot be used in saline environments (de Beer & van den Heuvel 1988, de Beer et al. 1997, Verschuren et al. 1999). Microscale biosensor technology, including lifetime and signal stability, is continuously being improved; for example, it is now possible to conduct microscale biosensor profiling in the deep-sea from self-contained landers (R. Glud et al. unpubl. data). In the future, such work will supplement our
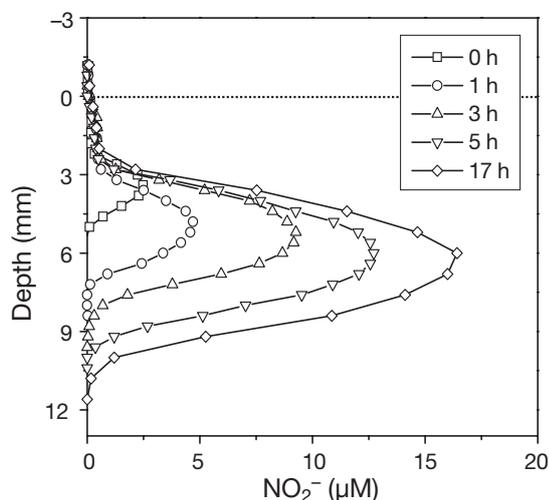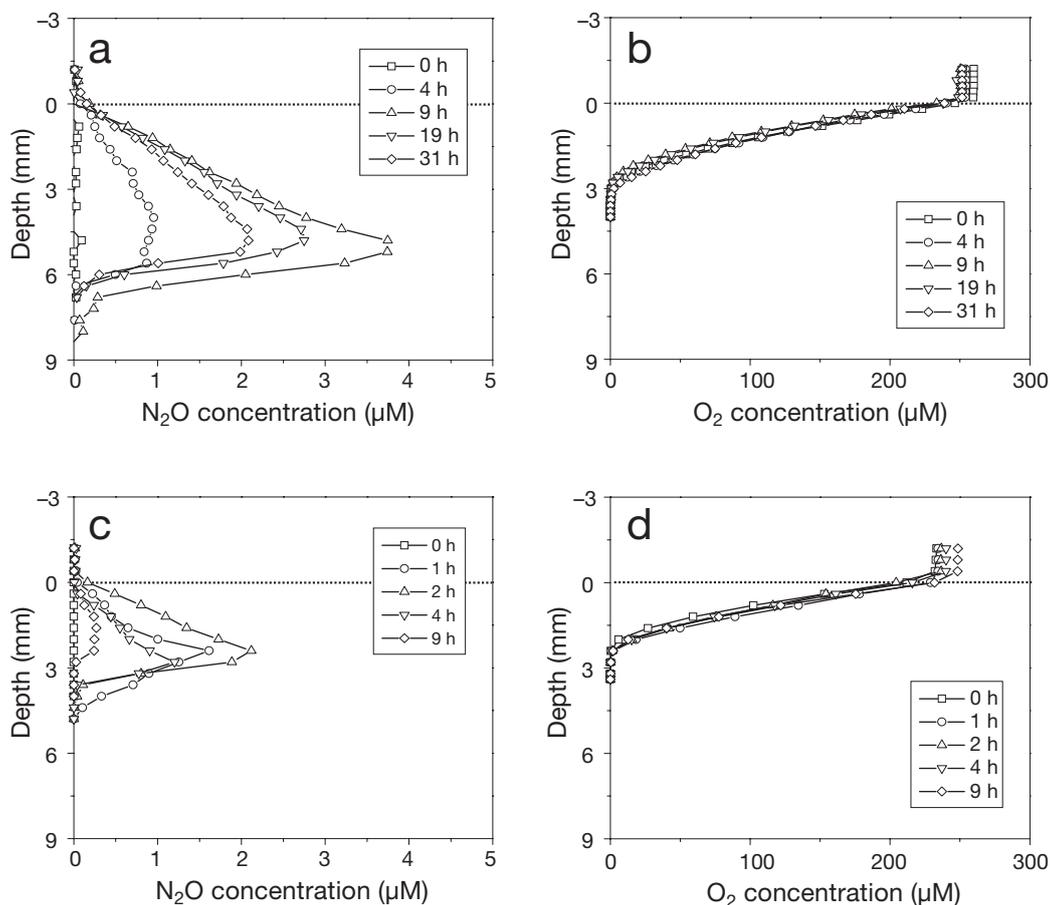

Fig. 6. Concentration profiles of NO_2^- in sediment from the brackish water site during transition from low (10 µM) to high (200 µM) NO_3^- concentration in the water phase, measured at 0, 1, 3, 5, and 17 h. Dotted line indicates sediment surface

Fig. 7. Concentration profiles of N_2O and O_2 in (a, b) freshwater and (c, d) marine sediments during salinity perturbation experiments. The freshwater sample was subject to a change from 0.5‰ salinity, 200 µM NO_3^- water to 6.5‰ salinity, 200 µM NO_3^- water. The marine sample was subject to a change from 25‰ salinity, 10 µM NO_3^- water to 6.5‰ salinity, 200 µM NO_3^- water. The dotted lines indicate the sediment surface

knowledge about nitrogen cycling in less accessible environments.

The concentration profiles were initially measured at conditions of 10 µM NO_3^- in the water phase, which is significantly lower than *in situ* concentrations, especially at the fresh- and brackish water sites. However, analyses at low NO_3^- concentrations allowed precise identification of nitrification zones in the sediment without the inaccuracy caused by a high NO_3^- background. Subsequently, NO_3^- concentrations were increased to 200 µM to study effects of NO_3^- supply to anoxic regions on anaerobic NO_2^- and N_2O dynamics. Finally, the metabolic potential of the nitrifying population in sediment from the brackish water site was examined by addition of NH_4^+. The rationale behind the perturbation experiments was to study the effects of naturally occurring fluctuations in salinity and NO_3^- on sediment N_2O dynamics at the brackish water site during tidal cycles and at the freshwater and marine sites during extreme weather events. If N_2O production is stimulated by salinity changes, sediments from

such areas may represent a significant atmospheric N_2O source. By investigating sediments along a gradient in tidal fluctuation, it was possible to elucidate whether the microbial communities can adapt to such a continuously changing chemical environment. It has previously been shown how changes in oxygen concentration in the water phase (Larsen et al. 1997) or changes in oxygen caused by benthic photosynthesis (Lorenzen et al. 1998) affect microprofiles of nitrification and NO_x^- respiration. However, due to the limitations imposed by the complexity of the microsensor array, we limited this investigation of nitrogen intermediate accumulation to the effects of changes in nitrogen availability and salinity. None of the investigated sites were subject to intense activity of burrowing infauna, but such fauna may have profound impacts on both nitrification (Kristensen et al. 1985) and denitrification (Binnerup et al. 1992), and thus on the formation of nitrogen intermediates, when they create a 3-dimensional network of oxic and anoxic sites.

Generally, intermediates can accumulate if subsequent steps in a sequence of conversions are limited by kinetics or by limited supply of a reactant. Microbial communities can respond quickly to kinetic limitations by gene induction, whereas cell growth is a slower process, especially for the NH_4^+ and NO_2^- oxidising populations. With our microsensor experiments, we aimed to elucidate whether and when either nitrification or denitrification can be responsible for nitrogen intermediate release and consumption.

NO_2^- dynamics

Significant variation in sediment NO_2^- dynamics was observed along the estuary, in terms of both accumulation and release patterns. The concentration profiles revealed NO_2^- production in both oxic and anoxic sediment layers, and hence showed examples of NO_2^- accumulation related to either aerobic or anaerobic processes. Although nitrification activity was high at all sites, the potential of the nitrifying community to further oxidise the produced NO_2^- to NO_3^- differed. In oxic layers of fresh- and brackish water sediments, the accumulation of NO_2^- was nearly absent, which contrasts the high level of NO_2^- accumulation in the marine sediment. The different scenarios may be partially explained by differences in NH_4^+ availability. In marine sediment, nitrification was evenly distributed throughout the oxic layer (low NO_3^- incubation), indicating that NH_4^+ availability was not process limiting. Indeed, the measured sediment NH_4^+ efflux exceeded the estimated NH_4^+ oxidation rates 3- to 6-fold. In contrast, the nitrification activity at fresh- and brackish water sites was primarily associated with the oxic–anoxic boundary, where NH_4^+ was likely supplied from the deep anoxic layers and fully oxidised. The presence of ammonium limitation in oxic surface layers was further confirmed for the brackish water site by the NH_4^+ addition experiment, which showed a greatly stimulated nitrifying activity that was distributed evenly throughout the oxic layer (Fig. 5). Accumulation of NO_2^- in the nitrification zone indicates an imbalance between the ammonia and nitrite oxidising communities, with a higher ammonia than NO_2^- oxidation rate. There may be historic reasons for the incomplete nitrification, such as a recent disturbance removing most of the oxic microbial community that, subsequently, must re-establish. The time period for a disturbed nitrifying community to re-establish itself may be >1 wk (Nielsen & Revsbech 1998), and the relative biomass increase of the 2 bacterial groups may depend on a multitude of factors, such as O_2, NH_4^+, and NO_2^- concentrations, pH, and temperature (Hellinga et al. 1998). According to the observed dynamics at our

3 sites, the anaerobic formation of NO_2^- in sediments appears to be highly variable. The variation along the estuary is probably related to differences in resident microbial populations in the sediment that are adapted to NO_3^- respiration. A positive correlation between NO_3^- availability and anaerobic NO_2^- production was observed in fresh- and brackish water sediments, as has also been reported for other systems (e.g. Stief et al. 2002).

The calculated rates of ammonia oxidation were 1.8 to 2.7× higher in incubations with 200 µM than with 10 µM NO_3^- (Table 3). Such a stimulating effect of increased NO_3^- availability on nitrification is rather surprising. It can be reasoned that NO_3^- addition to the water column results in enhanced DNRA in anoxic sediment zones, followed by increased nitrification activity in the overlying oxic zone due to upward NH_4^+ diffusion. However, such an explanation seems unlikely for the marine sediment, which, in contrast to fresh- and brackish water sediments with suspected NH_4^+ limitation, released significant amounts of NH_4^+. Determination of nitrifying activity in sediments by use of ^{15}N stable isotope techniques generally do not show increased rates of nitrification when the NO_3^- concentration is elevated (L. P. Nielsen pers. comm.). Hence, the consistent finding of higher ammonia oxidation rates after NO_3^- addition is likely an artefact of our calculation, with larger errors for the estimates at high water phase NO_3^- concentration. We were aware of this potential source of error while planning the experiment, as surface determinations and exact diffusivity determinations become critical with almost vertical surface NO_3^- profiles at high concentrations, and we therefore conducted additional experiments at artificially low NO_3^- concentrations. The inaccuracy at high concentrations is essentially the same problem as usually encountered when a small value is obtained by subtracting 2 large values. Ideally, the data would have been supplemented with microprofiles of NH_4^+, which would have helped in resolving this issue, but NH_4^+ microsensors do not function in saline environments.

Sediment release of NO_2^- to the water phase, as demonstrated in the present study, is regulated through interactions between aerobic and anaerobic transformation processes. From an environmental perspective, the production of NO_2^- in oxic sediment layers appears particularly critical, because it could give rise to high efflux rates (as observed in marine sediment) due to a short diffusion distance from the production zone to the sediment–water interface. In comparison, the effect of increased anaerobic NO_2^- formation on water column efflux is less predictable. Anoxic NO_2^- accumulation will lead to diffusion of NO_2^- into oxic sediment layers, which may act as a

NO_2^- sink, thus preventing the escape of anaerobically formed NO_2^- from the sediment surface. This occurred in fresh- and brackish water sediments, where all NO_2^- was consumed, most likely by NO_2^- oxidation. When NH_4^+ was supplied to the overlying water, the oxic zone of sediments from the brackish water site could no longer oxidise all NO_2^- produced, simply because the NO_2^- oxidising potential was then saturated by the combined oxic and anoxic NO_2^- supply. Because ammonium oxidisers in general cope better with low oxygen concentrations than nitrite oxidisers (Hanaki et al. 1990), reduced oxygen availability for sediment processes will proportionally reduce the effectiveness of the oxic layer as a NO_2^- sink, leading to increased sediment efflux of NO_2^- originating from the anoxic layers (Stief et al. 2002). The effect of microphytobenthos on NO_2^- release was not studied here, but it is likely that a cover of microphytobenthos would reduce the release. Microphytobenthos has been shown to reduce overall nitrification and thus NO_2^- production (Risgaard-Petersen 2003), likely due to competition for substrate.

N_2O dynamics

The production of N_2O varied along the Weser estuary but, characteristically, only transient sediment N_2O accumulation was observed. At the freshwater site, either increased NO_3^- concentration or elevated salinity caused N_2O accumulation. In subtropical Australian mangrove sediment, NO_3^- loading also induced N_2O accumulation; however, the increased production was not a transient phenomenon in this system, as high concentrations of N_2O (>12 µM) were detected over a period of 10 d (Meyer et al. 2008). The observed difference in temporal N_2O dynamics at the 2 locations may reflect that the mangrove sediment was exposed to a more dramatic perturbation, originating from a lower nutrient environment (*in situ* NO_3^- < 100 µM), and experimentally incubated with 500 µM NO_3^-. However, the stimulated formation of N_2O by NO_3^- occurred in anoxic layers in both sediments and was therefore related to anaerobic processes. In the respiratory pathway of denitrification, the induction of nitrous oxide reductase synthesis is often found to lag behind the induction of the other enzymes, which leads to a peak in N_2O formation at the onset of anoxic conditions or the addition of nitrate (Firestone & Tiedje 1979). The stimulated production of N_2O during an abrupt change in salinity likely reflects that either N_2O-reductases or populations specialized on N_2O reduction are salinity sensitive. In the marine sediment, transient accumulation of N_2O was only observed when the sediment was exposed to low salinity water with high NO_3^-. The production of N_2O hap-

pened just at the border of the oxic–anoxic zone, and it is therefore difficult (even with high resolution microprofiles) to conclude whether accumulation in this situation was related to activity of nitrifiers, denitrifiers, or both. This is in contrast to the microsensor work by Meyer et al. (2008), where a distinct oxic N_2O production zone (at high NH_4^+ conditions) was clearly identified and hence could be attributed to nitrification with higher certainty. It should be noted that it is difficult to isolate the causal factor for N_2O accumulation in the marine sediment in the present study. Because the transient dynamics were fast, it cannot be ruled out that a similar scenario also occurred when the NO_3^- concentration was increased from 10 to 200 µM (at constant salinity). Therefore, the accumulation of N_2O could be a response to the increased NO_3^- supply, rather than being a salinity effect.

N_2O oxide accumulation was, in all cases, observed to induce sediment release of N_2O to the overlying water phase. Thus, in contrast to NO_2^- dynamics, where NO_2^- oxidation in the aerobic layer might prevent release of anaerobically produced NO_2^- to the water phase, aerobic transformation of N_2O did not take place. Indeed, the only microbial process that consumes N_2O under oxic conditions is aerobic denitrification, which is rarely reported in natural samples (Robertson et al. 1995). Interestingly, almost equal N_2O efflux rates were found in the marine and freshwater samples during salinity perturbations (Table 2), although N_2O accumulated to an almost 2-fold higher concentration in the freshwater sediment (Fig. 7). The deeper location of the anoxic N_2O production zone and, consequently, longer diffusion path for N_2O to the sediment surface in the freshwater sample explains this situation, elegantly demonstrating the importance of diffusion distance on sediment release rate.

The significant contribution of estuarine environments to atmospheric N_2O is well recognized, but mechanistic insight is limited. Low salinity regions, rather than marine sites, have been identified as important areas for N_2O release (Robinson et al. 1998, Barnes & Owens 1999, De Bie et al. 2002). This correlates well with the results from the present study, where the highest N_2O efflux was observed from freshwater sediment. In the hypernutrified Colne Estuary, high N_2O release rates were found for tidal sediments that experience diurnal fluctuations in NO_3^- availability (Robinson et al. 1998). The transient N_2O release dynamics at our freshwater site (and possibly at the marine site) upon transition from low to high NO_3^- water indicate that fluctuation in NO_3^- availability represents an important mechanism of N_2O formation in the Weser estuary, as such variation is often encountered during the tidal cycles. Further, the demonstration of salinity-induced N_2O release from

Weser sediments suggests salinity as a potential causal factor of N_2O production, but the environmental significance of the observed dynamics remains to be addressed. Clearly, the naturally occurring tidally induced changes in salinity are usually slower and less extreme than the applied perturbations; therefore, our findings may not reflect *in situ* dynamics. As opposed to freshwater and marine sites that only experience fluctuations in salinity under more extreme weather conditions, the brackish water site experiences diurnal variations in salinity, hence representing the area of the estuary where salinity-induced N_2O production is most likely to constitute a major source. For this reason, we especially focused on N_2O dynamics at the brackish water site, exposing the sediment to a range of perturbations; however, the sediment proved highly resistant to N_2O accumulation. The absence of N_2O accumulation at this site may have been caused by adaptation of the resident microbial communities to the continuously changing ambient conditions; only the sites that were not regularly exposed to diurnal variations were sensitive to salinity perturbations.

CONCLUSIONS

The fluxes of NO_2^- and N_2O from estuarine sediments to the overlying water or atmosphere are governed by complex interactions between resident microbial populations and overlying water chemistry. In general, the processes that convert large amounts of NO_2^- and N_2O to their end-products are surprisingly well geared and, as such, perturbations in environmental factors usually only result in transient accumulations.

LITERATURE CITED

Andersen K, Kjær T, Revsbech NP (2001) An oxygen insensitive microsensor for nitrous oxide. Sens Actuators 81: 42–48

Bange HW, Rapsomanikis S, Andreae MO (1996) Nitrous oxide in coastal waters. Global Biogeochem Cycles 10: 197–207

Barnes J, Owens JP (1999) Denitrification and nitrous oxide concentrations in Humber Estuary, UK, and adjacent coastal zones. Mar Pollut Bull 37:247–260

Beddig S, Brockermann U, Dannecker W, Korner D and others (1997) Nitrogen fluxes in the German Bight. Mar Pollut Bull 34:382–394

Berg P, Risgaard-Petersen N, Rysgaard S (1998) Interpretation of measured concentration profiles in sediment pore water. Limnol Oceanogr 43:1500–1510

Betlach MR, Tiedje JM (1981) Kinetic explanation for the accumulation of nitrite, nitric-oxide, and nitrous-oxide during bacterial denitrification. Appl Environ Microbiol 42:1074–1084

Binnerup SJ, Jensen K, Revsbech NP, Jensen MH, Sørensen J (1992) Denitrification, dissimilatory reduction of nitrate to ammonium, and nitrification in abioturbated estuarine sediment as measured with ^{15}N and microsensor techniques. Appl Environ Microbiol 58:303–313

Broecker WS, Peng TH (1974) Gas-exchange rates between air and sea. Tellus 26:21–35

Conrad R (1996) Soil microorgansims as controllers of atmospheric trace gases (H_2, CO, CH_4, OCS, N_2O, and NO). Microbiol Rev 60:609–640

de Beer D, van den Heuvel JC (1988) response of ammonium-selective microelectrodes based on the neutral carrier nonactin. Talanta 35:728–730

de Beer D, Schramm A, Santegoeds CM, Kuhl M (1997) A nitrite microsensor for profiling environmental biofilms. Appl Environ Microbiol 63:973–977

de Bie MJM, Middelburg JJ, Starink M, Laanbroek H (2002) Factors controlling nitrous oxide at the microbial community and estuarine scale. Mar Ecol Prog Ser 240:1–9

Dong LF, Nedwell DB, Underwood GJC, Thornton DCO, Rusmana I (2002) Nitrous oxide formation in the Colne estuary, England: the central role of nitrite. Appl Environ Microbiol 68:1240–1249

European Economic Community (1978) A directive of the quality of freshwater needing protection or improvement in order to support fish life. Off J Eur Comm 222:34–54

Firestone MK, Tiedje JM (1979) Temporal change in nitrous oxide and dinitrogen from denitrification following onset of anaerobiosis. Appl Environ Microbiol 38:673–679

Grabemann I, Uncles RJ, Krause G, Stephens JA (1997) Behavior of turbidity maxima in the Tamar (UK) and Weser (FRG) Estuaries. Estuar Coast Shelf Sci 45: 235–246

Hanaki K, Wantawin C, Ogaki S (1990) Nitrification at low levels of dissolved oxygen with and without organic loading in a suspended-growth reactor. Water Res 24:297–302

Hellinga C, Schellen AAJC, Mulder JW, van Loosdrecht MCM, Heijnen JJ (1998) The SHARON process: an innovative method for nitrogen removal from ammonium-rich waste water. Water Sci Technol 37:135–142

Holtan-Hartwig LP, Dörsch P, Bakken LR (2000) Comparison of denitrifying communities in organic soils: kinetics of NO_3^- and N_2O reduction. Soil Biol Biochem 32:833–843

Keeney DR, Nelson DW (1982) Nitrogen: inorganic forms. In: Page AL (ed) Methods of soil analysis. American Society of Agronomy, Madison, WI, p 643–693

Kelso BHL, Smith RV, Laughlin RJ, Lennox SD (1997) Dissimilatory nitrate reduction in anaerobic sediments leading to river nitrite accumulation. Appl Environ Microbiol 63: 4679–4685

Kelso BHL, Glass DM, Smith RV (1999b) Toxicity of nitrite to freshwater invertebrates. In: Wilson WS, Ball AS, Hinton RH (eds), Managing risk of nitrates to humans and the environment. Royal Society of Chemistry, Cambridge, p 175–188

Kjær T, Larsen LH, Revsbech NP (1999) Sensitivity control of ion-selective biosensors by electrophoretically mediated analyte transport. Anal Chim Acta 391:57–63

Kramlich JC, Linak WP (1994) Nitrous oxide behaviour in the atmosphere, and in combustion and industrial systems. Prog Energy Combust Sci 20:149–202

Kristensen E, Jensen MH, Andersen TK (1985) The impact of polychaete (*Nereis virens* Sars) burrows on nitrification and nitrate reduction in estuarine sediments. J Exp Mar Biol Ecol 85:75–91

Larsen LH, Kjær T, Revsbech NP (1997) A microscale NO_3^- biosensor for environmental applications. Anal Chem 69: 3527–3531

Laursen AE, Seitzinger SP (2004) Diurnal patterns of denitrifi-

cation, oxygen consumption and nitrous oxide production in rivers measured at the whole-reach scale. Freshw Biol 49:1448–1458

Li YH, Gregory S (1974) Diffusion of ions in sea water and in deep-sea sediments. Geochim Cosmochim Acta 38: 703–714

Lorenzen J, Larsen LH, Kjær T, Revsbech NP (1998) Biosensor determination of the microscale distribution of nitrate, nitrate assimilation, nitrification, and denitrification in a diatom inhabited freshwater sediment. Appl Environ Microbiol 64:3264–3269

Meyer RL, Risgaard-Petersen N, Allen DE (2005) Correlation between anammox activity and microscale distribution of nitrite in a subtropical mangrove sediment. Appl Environ Microbiol 71:6142–6149

Meyer RL, Allen DE, Schmidt S (2008) Nitrification and denitrification of sediment nitrous oxide production: a microsensor approach. Mar Chem 110:68–76

Naqvi SWA, Jayakumar DA, Narvekar PV, Naik H and others (2000) Increased marine production of N_2O due to intensifying anoxia on the Indian continental shelf. Nature 408: 346–349

Neumann D, Kramer M, Raschke I, Grafe B (2001) Detrimental effects of nitrite on the development of benthic *Chironomus* larvae, in relation to their settlement in muddy sediments. Arch Hydrobiol 153:103–128

Nielsen TH, Revsbech NP (1998) Nitrification, denitrification, and N-liberation associated with two types of hot-spots in soil. Soil Biol Biochem 30:611–619

Nielsen M, Larsen LH, Jetten MSM, Revsbech NP (2004) Bacterium-based NO_2^- biosensor for environmental applications. Appl Environ Microbiol 70:6551–6558

Ogilvie B, Nedwell DB, Harrison RM, Robinson A, Sage A (1997) High nitrate, muddy estuaries as nitrogen sinks: the nitrogen budget of the River Colne estuary (United King-

dom). Mar Ecol Prog Ser 150:217–228

Philips S, Laanbroek JH, Verstraete W (2002) Causes and effects of increased nitrite concentrations in aquatic environments. Environ Sci Technol 1:115–141

Revsbech NP (1989) An oxygen microelectrode with a guard cathode. Limnol Oceanogr 34:472–476

Revsbech NP, Nielsen LP, Ramsing NB (1998) A novel microsensor for the determination of diffusivity in sediments and biofilms. Limnol Oceanogr 45:986–992

Risgaard-Petersen N (2003) Coupled nitrification-denitrification in autotrophic and heterotrophic estuarine sediments: on the influence of benthic microalgae. Limnol Oceanogr 48:93–105

Robertson LA, Dalsgaard T, Revsbech NP, Kuenen JG (1995) Confirmation of 'aerobic denitrification' in batch cultures, using gas chromatography and ^{15}N mass spectrometry. FEMS Microbiol Ecol 18:113–120

Robinson AD, Nedwell DB, Harrison RM, Ogilvie BG (1998) Hypernutrified estuaries as sources of N_2O emission to the atmosphere: the estuary of the River Colne, Essex, UK. Mar Ecol Prog Ser 164:59–71

Stief P, De Beer D, Neumann D (2002) Small-scale distribution of interstitial nitrite in freshwater sediment microcosms: the role of nitrate and oxygen availability, and sediment permeability. Microb Ecol 43:367–378

Venterea RT, Rolston DE (2000) Mechanistic modeling of nitrite accumulation and nitrogen oxide gas emissions during nitrification. J Environ Qual 29:1741–1751

Verschuren PG, van der Baan JL, Blaauw R, de Beer D, van den Heuvel JC (1999) A nitrate selective microelectrode based on a lipophilic derivative of iodocobalt(III)salen. Fresenius J Anal Chem 364:595–598

Wrage N, Velthof GL, van Beusichem ML, Oenema O (2001) Role of nitrifier denitrification in the production of nitrous oxide. Soil Biol Biochem 33:1723–1732